Published in final edited form as:
Nanoscale. 2012 January 21; 4(2): 330–342. doi:10.1039/c1nr11277e.

Theranostic nanoplatforms for simultaneous cancer imaging and therapy: current approaches and future perspectives

Ki Young Choi, **Gang Liu**, **Seulki Lee**, and **Xiaoyuan Chen**
Laboratory of Molecular Imaging and Nanomedicine (LOMIN), National Institute of Biomedical Imaging and Bioengineering (NIBIB), National Institutes of Health (NIH), Bethesda, MD, 20892, USA

Seulki Lee: Seulki.Lee@nih.gov; Xiaoyuan Chen: Shawn.Chen@nih.gov

Abstract

Theranostics is a concept which refers to the integration of imaging and therapy. As an evolving new field, it is related to but different from traditional imaging and therapeutics. It embraces multiple techniques to arrive at a comprehensive diagnostic, *in vivo* molecular images and an individualized treatment regimen. More recently, there is a trend of tangling these efforts with emerging materials and nanotechnologies, in an attempt to develop novel platforms and methodologies to tackle practical issues in clinics. In this article, topics of rationally designed nanoparticles for the simultaneous imaging and therapy of cancer will be discussed. Several exemplary nanoparticle platforms such as polymeric nanoparticles, gold nanomaterials, carbon nanotubes, magnetic nanoparticles and silica nanoparticles will be elaborated on and future challenges of nanoparticle-based systems will be discussed.

1. Introduction

Cancer is the second leading cause of death in the United States. The National Cancer Institute estimates that more than 1,500 Americans die of cancer every day, and approximately 600,000 patients with cancer will die in 2011.[1] Given that this considerable mortality is primarily due to cancer metastasis to other organs, early detection is crucial for the effective management of cancer. For instance, the survival rate of patients with lung and bronchus cancer, which is the single leading cause of cancer-related death, is approximately 53% if the cancer is detected at an early stage before metastasis to distant tissues, organs or lymph nodes occurs. However, the survival rate significantly decreases to 4% when the cancer is detected in the late stage, *i.e.* after it metastasizes to distant tissues.[2] Although huge advances have been made in diagnostic technologies, a considerable portion of cancer patients are still diagnosed with metastases due to the poor selectivity and sensitivity of conventional diagnostic techniques.

Current treatment options applicable to metastatic cancers are still confined to chemotherapeutics with combinational regimens. Over the past several decades, considerable efforts have been directed towards the development of potent therapeutic agents. Yet, current anticancer therapeutics is limited in safety and efficacy. Most conventional anticancer agents show a narrow therapeutic window because they are randomly distributed in the whole body following administration. Non-specific biodistribution may cause cytotoxicity to normal and cancer cells alike, which causes severe

Correspondence to: Seulki Lee, Seulki.Lee@nih.gov; Xiaoyuan Chen, Shawn.Chen@nih.gov.

side effects to achieve sufficient anti-cancer efficacy. The non-specific toxicity of anticancer drugs also limits an injectable dose and thus lessens the therapeutic efficacy.

In an attempt to overcome these major hurdles in the treatment of cancer, various nanoparticle platforms have been extensively developed for cancer diagnostics and therapeutics. Nanoplatforms hold great potential in cancer diagnostics and therapeutics. Given sophisticated nano-structures and huge surface area to volume ratios, nanoparticles can accomodate a variety of diagnostic or therapeutic agents *via* chemical conjugation or physical encapsulation.[3] Moreover, nanoparticles are known to target tumors *via* passive accumulation and/or active-targeting approaches. Combining their capabilties to carry various cargos and to target tumors, they can be employed as targeted cancer diagnostics and therapeutics to get high-quality images indicating the tumor site and to achieve the enhanced therapeutic efficacy without severe cytotoxicity to normal cells. For these reasons, theranostic nanoparticles, a platform for both diagnostic and therapeutic functions, have been explosively investigated as a next-generation nanocarrier system.[4–8]

Theranostics is a term originally coined to define an approach that combines diagnostics with therapeutics.[9] It embraces multiple techniques to arrive at comprehensive diagnosis, molecular images and an individualized treatment regimen.[10–13] Recently, there is an effort to tangle the emerging approach with nanotechnologies, in an attempt to develop theranostic nanoplatforms and methodologies.[14] Given that cancer is a highly heterogeneous and adaptable disease, diverse types of treatment options need to be chosen depending on patient characteristics and disease progression. Cancer researchers hope that theranostic nanoparticles provide patients with various treatment options that are suitable for individuals, and thereby result in improved prognoses. Furthermore, theranostic nanoparticles can monitor therapeutic efficacy following treatments which can expedite clinician's individualized therapeutic decisions.

In this article, we will review various types of theranostic nanoplatforms including magnetic nanoparticles, carbon nanotubes, gold nanostructures, polymeric nanoparticles, and silica nanoparticles and discuss their applications in cancer theranostics. A number of review articles describe nanoparticle-based diagnostic or therapeutic systems for the treatment of cancer;[3,15,16] however, few articles have focused on theranostic nanoparticles capable of simultaneously imaging and treating cancer. Thus, this review will focus on nanoparticle systems that integrate tumor imaging and therapy into a single system. In detail, we will discuss theranostic applications of diverse nanoplatforms categorized by different nanomaterials such as polymeric, gold, carbon, magnetic and silica nanomaterials. These applications include: 1) diagnostics for the assessment of intracellular localization and *in vivo* biodistribution, 2) therapeutics for the treatment, and 3) theranostics for monitoring biological responses and therapeutic efficacy following treatment. Finally, we will address the limitations and future challenges of current theranostic systems based on diverse nanoplatforms.

2. Nanoplatforms

Nanoparticle-based theranostic systems exploit diverse nanoplatforms, *e.g.* magnetic nanoparticles, carbon nanotubes, gold nanostructures, polymeric nanoparticles, or silica nanoparticles. Interestingly, some types of nanoparticles, *e.g.* gold nanoshells/nanorods or carbon nanotubes absorb light energy and then scatter or emit specific types of diagnostic/therapeutic signals, *e.g.* ultrasound, heat, Raman or fluorescence signals. These types of nanoparticles can function as theranostic nanoparticles on their own. However, in general, nanoplatforms are modified with additional diagnostic and therapeutic agents so as to function as theranostic nanoparticles. The nanoplatforms are chemically or physically

labeled with radionuclides, MRI agents, or optical imaging agents. Simultaneously, anticancer agents including hydrophobic chemical drugs, peptides, proteins, or genetic drugs are physically encapsulated into or chemically conjugated onto the nanoparticles. We summarize the representative nanoplatforms in Table 1.

In particular, nanoparticles have been known to target tumors *via* passive- and/or active-targeting pathways. Due to abnormally leaky vasculature and lack of an effective lymphatic drainage system in tumor tissues, nanoparticle platforms can passively accumulate into the tumor tissues. These unique phenomena are jointly referred to as the enhanced permeation and retention (EPR) effect. Moreover, the nanoparticles can recognize, bind to, and internalize into tumor cells *via* receptor-mediated endocytosis when modified with tumor-targeting moieties such as antibodies,[67–69] nucleic acids,[70,71] proteins,[72–75] or other ligands.[76–78] In this section, we will describe exemplary theranostic nanoplatforms and also discuss their applications in cancer.

2.1. Magnetic nanoparticles

Magnetic nanoparticles, especially iron oxide nanoparticles (IONPs), are an important class of biomaterials and are used for various purposes, such as imaging,[79] cell labeling,[28,30,80] drug delivery,[81] gene delivery[21] and hyperthermia.[26] IONPs, possessing substantial saturation magnetization values at room temperature, are nanocrystals made from magnetite or hematite. The popularity of IONPs in theranostics is mainly because: 1) IONPs have been the most prominent transverse relaxation time (T_2)/T_2^* among contrast agents for magnetic resonance imaging (MRI).[82] IONPs can shorten T_2 relaxation time and bring negative contrast, resulting in hypointense images to monitor small pathological changes and drug delivery *in vivo*; 2) like other NPs, IONPs have a large surface area for carrying various biomolecules and drugs.[79] Well-developed surface chemistry allows fine control of the physical properties of IONPs, including size, surface charge, crystal structure, and magnetic properties; 3) IONPs can play attractive imaging/therapy dual roles in cancer treatment, due to its potential in hyperthermia;[34] 4) IONPs exhibit excellent biosafety because they can be degraded and metabolized into the serum Fe pool to form hemoglobin or to enter other metabolic processes.[83]

A good example of IONP-based theranostics is the IONP-doxorubicin (DOX)-cRGD micelles, reported by Nasongkla *et al.*[60] in 2006. They simultaneously loaded DOX and IONPs into the cores of poly(ethylene glycol)-poly(D,L-lactide) (PEG-PLA) micelles. In addition, the targeting modality, a cyclic Arginine-Glycine-Aspartic Acid (cRGD) ligand, was functionalized onto the micelle surface to target the integrin $a_v\beta_3$ found on tumors or endothelial cells. The probes's integrated capability to be used as MR imaging agents and as drug delivery vehicles, make them a good candidate for future cancer diagnosis and therapy. Similarly, Yu *et al.*[20] successfully loaded DOX into anti-biofouling polymer coated IONPs. The DOX loaded IONPs showed better pharmacokinetics and therapeutic effects than DOX alone in a Lewis lung carcinoma xenograft model, presumably due to the anti-biofouling effect of the IONPs. Additionally, IONPs with appropriate coatings can be easily coupled with drug molecules. More recently, our group demonstrated a theranostic application using IONPs coated with human serum albumin (HSA), which has been considered a biocompatible matrix material for chemotherapeutics,[84,85] photosensitizers[86] and NPs.[29,30,35] These IONPs, coated with dopamine and HSA (HINPs), achieved tumor targeting *via* passive means.[29] In addition, therapeutics such as DOX were co-loaded into dopamine-HSA matrices.[35] DOX-incorporated HINPs (D-HINPs) exhibited excellent tumor-targeting, which was used to clearly visualize the tumor site *in vivo* by MRI in real time (Fig. 1). Simultaneously, intravenous administration of D-HINPs greatly outperformed free DOX to significantly suppress tumor growth. Interestingly, the antitumor efficacy of D-HINPs was comparable to Doxil, a liposome-based DOX formula used in the clinic for the

treatment of various cancer types. Therefore, D-HINP can be a promising theranostic nanoplatform for simultaneous cancer imaging and therapy.

Drug molecules can also be loaded into porous IONPs *via* physical absorption. Hyeon group performed "wrap-bake-peel" process, which first wraps the IONPs with a silica coating, heats the conjugates and finally removes the silica layer, to achieve water-dispersible and biocompatible hollow IONPs.[19] DOX could be loaded into the hollow IONPs by simple physical absorption and then released from the nanostructures in a sustained manner under physiologic conditions. In another example, Cheng *et al.*[22] reported porous hollow IONPs as a cisplatin delivery vehicle for target-specific therapeutic applications. The porous IONPs with a sizable cavity were achieved by controlling oxidation and acid etching of IONPs. Cisplatin was loaded into the cavities of the IONPs and Herceptin (HER2 monoclonal antibody) was coupled onto the IONPs surfaces to confer targeting specificity. The resulting IONPs showed selective affinity to breast cancer cells and a sustained cytoxicity attributable to the controlled release of cisplatin from the IONPs.

Unlike small drug molecules, which are usually able to diffuse across cell membranes, biomolecules such as proteins or therapeutic genes cannot penetrate the cell membrane due to their large molecular weight or negative surface charge and thus require delivery carriers for cellular entry.[87] Transportation of gene into cells *via* IONPs was achieved,[79,87] where it was shown that genes could either be conjugated or noncovalently absorbed on IONPs for intracellular delivery. In an ideal situation, the IONP carriers can load the therapeutic genes, escort them to the diseased tissues, and facilitate their shuttling across the cell membranes. Later on, in the endosomes/lysosomes, where the pH is lower, the DNA/siRNA cargos are released due to the proton sponge effect and then fulfill their functions. In the milestone work reported by Medarova *et al.*,[17] Multifunctional IONPs for simultaneous *in vivo* imaging and siRNA delivery into tumors have been developed. Thiolated siRNA was coupled onto aminated dextran particles using *N*-succinimidyl-3-(2-pyridyldithio) propionate (SPDP) as a bridge compound. In addition, myristoylated poly-arginine peptide (MPAP), a membrane translocation peptide, and the near infrared dye Cy5.5 were coupled to IONPs surface (Fig. 2). By tracking these probes *in vivo* by MR and NIR fluorescence imaging, functional IONPs could simultaneously deliver siRNAs and monitor therapeutic efficacy.

In our recent studies, we found that alkylated amphiphilic PEI is able to encapsulate one or multiple IONPs and form stable composites with good magnetic properties and biocompatibility in aqueous environment.[88–90] Low molecular weight N-alkyl-PEI_{2k} capped IONPs possess many outstanding features that favor siRNA delivery,[33] including high siRNA binding capability, protection of siRNA from enzymatic degradation, and ability to release complexed siRNA in the presence of poly-anionic heparin. When loaded with siRNA, Alkyl-PE_{I2k}-IONPs induced gene silencing effects at both the *in vitro* and *in vivo* levels with good biocompatibility. Meanwhile, the transfected cells displayed strong signal contrast compared to untreated cells on T_2 weighted imaging. This multifunctional nanocomposite system provides a safe and efficient method for gene delivery with non-invasive imaging capability. The magnetic properties of IONPs allow them to accumulate upon the summons of an external magnetic field, which has been utilized as a targeting mechanism to improve drug delivery efficiency. Namiki *et al.*[24] loaded siRNA onto cationic lipid coated IONPs and evaluated the therapeutic potency in two gastric cancer models. They demonstrated the gene silencing effects was only significant during application of magnetic fields at the tumor sites. In a very recent effort,[91] Mikhaylov *et al.* also demonstrated that IONPs clusters encapsulated inside a liposome can target both a mammary tumor and its microenvironment in a mouse under the influence of an external magnet. The targeting of the tumor microenvironment by the drug-loaded ferriliposomes

was non-invasively monitored *in vivo*, resulting in a significant reduction in tumor growth. Such IONP-based, multifunctional MRI-visible targeted delivery systems show great potential for the diagnosis and treatment of cancer.

2.2. Carbon nanotubes

Unique physical and chemical properties of carbon nanotubes (CNTs) have been widely explored in the field of Raman and photoacoustic imaging and drug delivery.[92–95] CNTs are low-dimensional sp^2 carbon nanomaterials and are categorized as single-walled carbon nanotubes (SWCNTs) and multi-walled carbon nanotubes (MWCNTs), where SWCNTs are made up of a single rolled up layer of a graphene sheet and MWCNTs consist of multiple rolled layers (concentric tubes of SWCNTs) of graphene. Typical diameters of SWCNTs are less than 5 nm; while for MWCNTs, the diameter can be around 100 nm. CNT length can vary from hundreds of nanometres up to tens of micrometres. The graphene structure that makes up the CNT is inert and applicable to most conjugation chemistry. The graphene wall can be functionalized with various biomolecules, imaging agents, and drugs *via* either covalent conjugation or non-covalent adsorption.[96] Generally, covalently conjugated drug molecules such as paclitaxel and cisplatin are linked to the functional groups on the CNTs surface or to the polymer coating of CNTs *via* cleavable bonds.[46,97] PEGylated phospholipids is one of the most studied ligands that are available to functionalize the CNTs surface. PEG confers on CNTs several important properties such as high solubility and stability, biocompatibility, and prolonged blood circulation time.[94,98] The aromatic stacking nature of CNTs surface also encourages non-covalent molecule anchoring. For example, aromatic molecules with a flat structure such as DOX can be absorbed on the surface of PEGylated SWCNTs *via* non-covalent π–π stacking.[99]

The unique physical properties of CNTs are advantageous for use as theranostics due to the strong optical absorption in the NIR regions.[95,96] Upon irradiation with NIR light, CNTs generate heat *via* light absorption and induce thermal destruction of cancer cells containing CNTs.[45] Bhirde *et al.*[95] reported that the unique Raman properties of CNTs in combination with a portable handheld device can be used to create a theranostic platform for cancer therapy. Both SWCNTs and MWCNTs can diffuse into and be taken up by ovarian cancer cells grown in two-dimensional cell culture or three-dimensional environment. They can be selectively irradiated and detected in cancer cells using a simple handheld Raman instrument. The MWCNTs have a higher thermal generation capacity but are harder to detect because of the low Raman signal intensity. SWCNTs provide a more suitable theranostic platform, because not only can they raise cellular temperatures but are also easily detected. Moon *et al.*[100] demonstrated that the combined treatments of SWNT and NIR irradiation led to the eradication of tumors with no observation of recurrence over six months in a human epidermoid mouth carcinoma model. Similarly, Liu *et al.*[101] reported that *in vivo* photothermal tumor ablation was achieved using SWCNT conjugates after intravenous injection followed by NIR laser irradiation.

Robinson *et al.*[44] demonstrated the first dual application of intravenously-injected SWCNTs as photoluminescent agents for *in vivo* tumor imaging and as NIR absorbers for photothermal therapy (Fig. 3). SWCNT distribution within tumors was tracked at a high spatial resolution due to their intrinsic optical properties and highly effective tumor elimination was achieved for large numbers of photothermally treated mice with good biocompatiblity. This example highlights the promise of utilizing the intrinsic optical properties of SWCNTs for *in vivo* imaging-guided photothermal cancer therapy. CNTs have also been found to form stable complexes with plasmid DNA/siRNA for the successful delivery of genes.[102–104] Bartholomeusz *et al.*[104] reported that pristine SWCNTs could be noncovalently bound to siRNA, which served as the cargo to silence hypoxia-inducible factor 1 alpha (HIF-1α) as well as the suspending agent for SWCNTs. The complex was

intratumorally administered into mice bearing pancreatic tumors with a HIF-1α/luciferase reporter and the gene silence effects were demonstrated using bioluminescence imaging.

CNTs are easily functionalized and can shuttle various payloads such as drug molecules, NIRF dyes, radio isotopes, magnetic nanoparticles and gold nanoparticles. In addition, they generate therapeutic thermal energy in response to NIR laser. They can also produce photoacoustic or photoluminescence signals for cancer imaging. For these reasons, they have been regarded as a versatile nanoplatform for cancer theranostics. However, their non-biodegradability has widely raised concern of safety. Recently, it was reported that CNTs potentially induce chronic diseases such as inflammation, fibrosis or lung cancer in mice.[105–108] Therefore, to use CNTs in clinical settings, the safety issues should be the priority.

2.3. Gold nanomaterials

Gold-based nanomaterials (GNMs) have emerged as a theranostic nanoplatform.[109,110] Since GNMs are bio-inert and can be easily modified with various biomolecules or chemical moieties, they have been widely used as nanoplatforms suitable for various biomedical applications. One of the most attractive attributes of GNMs is the tunable optical properties that mediate the localized surface plasmon resonance. Upon irradiation with light of an appropriate wavelength, GNMs show distinctive interactions; the incoming light is re-radiated at the same wavelength by scattering and is also converted into vibrations of the lattice by absorption, generating heat energy. Upon irradiation, GNMs also induce strong electric fields on the surface of the particles. Depending on their size, shape and dielectric environments, the surface plasmon resonance can be controlled.[111] Recently, considerable efforts have been made to develop GNMs that show surface plasmon resonance at the near infrared (NIR) region, which is a tissue transparency window ideal for optical imaging and photothermal therapy, by changing their aspect ratio or tuning the wall thickness of GNMs. The efforts finally led to the development of unique gold nanoparticles (GNPs) such as gold nanoshells, gold nanorods or gold nanocages that can be excited in relatively deeper tissues *via* NIR irradiation, inducing backscattering signals and heat energy. Based on these unique properties, GNMs have been employed as contrast agents for diverse bioimaging modalities, *i.e.* dark-field, photoacoustic (PA) and optical coherence tomography (OCT) imaging. In addition, they have been harnessed as effective therapeutic agents for drug/gene delivery systems or photothermal therapy. Therefore, GNMs have been recently developed as multifunctional nanoplatforms in cancer theranostics.

West and co-workers first applied gold nanoshells (GNSs) that consist of a dielectric core surrounded by a thin gold shell to hyperthermal cancer therapy.[112] In the early study, they synthesized GNSs that have strong absorbance at the NIR spectral region by controlling the thickness of the gold shell and the size of the dielectric silica core. They also demonstrated the photothermal efficacy of GNSs in breast carcinoma animal models. Upon exposure to NIR light (820 nm, 4 W cm^{-2}, 5-mm spot diameter, <6 min), the temperature at the tumor site significantly increased ($\Delta T = 37.4 \pm 6.6$ °C), inducing irreversible tissue damage; whereas in the control mice treated with saline, negligible temperature increase was detected. In a follow-up study, they demonstrated theranostic applications of GNSs for dark-field imaging and photothermal therapy. In the study, they modified the GNSs with HER2 antibody, a targeting molecule that can bind to HER2 receptors overexpressed on breast carcinoma cells.[36] After incubating with SKBR3 breast cancer cells, effective binding of HER2-conjugated GNSs (HER2-GNSs) onto the cancer cells was visualized using a scatter-based darkfield imaging technique. Furthermore, upon irradiation with a NIR-emitting laser, the breast cancer cells incubated with HER2-GNSs were significantly destructed by the photothermal effect. The same group extended the applications of GNSs to *in vivo* OCT imaging and photothermal therapy (Fig. 4).[37] They prepared PEG-conjugated GNSs that can

strongly absorb NIR light and scatter, providing optical contrast signals for OCT bioimaging and heat energy for photothermal therapy simultaneously. After intravenous injection into CT-26 colon cancer-bearing mice, they obtained significantly stronger OCT signals in tumor tissues compared to those in normal tissues, showing passive accumulation in the tumor tissue. Following NIR irradiation, effective ablation of the tumor and an increase in survival rate of mice was observed in the GNSs treated mice as compared with those in the control group.

Combined with diverse types of imaging agents such as NIR fluorophores and magnetic nanomaterials, multifunctional GNS systems have been developed for multimodal imaging and photothermal therapy. Hyeon and co-workers describe the application of multifunctional magnetic gold nanoshells (MGNSs), comprised of a silica core (100 nm) surrounded with 15 nm-thick gold shell embedded with magnetic nanoparticles (7 nm) (Fig. 5).[113] To endow the MGNSs with specific targetability to epidermal growth factor receptors (EGFR) on the cancer cells, they further modified the surface with HER2 antibody. Upon incubation of HER2-MGNSs with HER2-positive SKBR3 breast cancer cells, high contrast MR signals were detected in SKBR3 cells. Following short exposure to NIR femtosecond laser pulses, cancer cells treated with HER2-MGNSs were rapidly destroyed by the photothermal effect. Chen *et al.*[114] described a nanoparticle system composed of a silica core embedded with Fe_3O_4 nanoparticles surrounded with a gold shell containing a fluorophore indocyanin green (ICG) for dual modal imaging and photothermal therapy. The surface of the fusion nanoparticles were modified with HER2 antibodies for specific tumor-targeting. MR and NIR fluorescence imaging exhibited specific binding of the HER2-conjugated nanomaterials to HER2-overexpressing and drug-resistant ovarian cancer OVCAR3 cells. Moreover, irradiation with an NIR laser led to photothermal ablation of cancer cells.

Besides GNS-based nanoplatforms, gold nanorods (GNRs)[40,115] and gold nanocages (GNCs)[116–118] have been extensively employed as cancer theranostics. Huang *et al.*[40] demonstrated the theranostic applications of GNRs for cancer cell imaging and photothermal cancer therapy (Fig. 6). They synthesized GNRs with a suitable aspect ratio of 3.9, which correspond to emission in the NIR region. The GNRs were modified with anti-epidermal growth factor receptor (anti-EGFR) monoclonal antibodies. When incubated with two malignant oral epithelial cell lines (HOC 313 clone 8 and HSC 3) and a nonmalignant epithelial cell line (HaCat), the significant signals for GNRs were detected on the cellular membrane of the malignant cell lines only. Consequently, the malignant cells were clearly delineated, whereas the nonmalignant cells were not clearly distinguished from background in dark field images. Upon irradiation of a continuous red laser at 800 nm, the malignant cells were photothermally destroyed by the relatively weaker laser power than that required for the destruction of nonmalignant cancer cells. In the malignant cells, significant damages were detected at 80 mW (10 W cm^{-2}), whereas in nonmalignant cells, any significant changes were not detected by 120 mW (15 W cm^{-2}). At 160 mW (20 W cm^{-2}), obvious damages were found in both cell types. GNCs have been recently explored as a potential theranostic nanoplatform due to their unique optical/physical attributes. Combined with the given optical properties of GNMs, the hollow nanostructure of GNCs offers new capabilities to hold hydrophilic drugs.[118] Furthermore, given that the drug-release from GNCs can be triggered by external signals such as a NIR laser or high-intensity focused ultrasound (HIFU), they can be employed as a smart drug delivery system. A recent study described the synthesis and application of GNCs for PA imaging and controlled drug delivery.[117] The GNCs contained the phase-change material (PCM), 1-tetradecanol, that has a melting point of 38–39 °C along with a fluorescence dye that acted a model drug. Since the PCMs can melt over 39 °C, the direct heating facilitated release of the dye molecules. Likewise, upon exposure to HIFU, the release of dyes was not only accelerated but controlled by HIFU power and/or exposure time.

Due to the unique characteristics, *i.e.* surface plasmon absorption, safety and ease of modification, various gold nanostructures have been considered an excellent nanoplatform for cancer theranostics. In particular, gold nanomaterials can themselves function as cancer theranostics for diagnostic imaging and therapy. However, they still pose hurdles in their clinical application. An intrinsic disadvantage of GNMs is the high cost of production. The other is an issue of stability in physiological conditions. Although thiol-gold surface chemistry has been employed to prepare diversely functionalized GNMs, it can be unstable in living substrata where glutathione is abundant. For clinical translation of GNMs, more stable surface chemistry is greatly required.

2.4. Polymeric nanoparticles

Polymeric nanoparticles are extensively used as an effective nanocarrier system for tumor imaging and therapy because: 1) their physicochemical properties such as particle size, surface charge or degradation rate are easily controlled, 2) their surface is easily modified with various targeting molecules, and 3) they can also shuttle various types of therapeutic agents or imaging probes.[15,119] With the advent of theranostics, multifunctional polymeric nanoparticles with integrated functions for cancer diagnostics and therapeutics have been vigorously developed.[14,16,120] One of the earliest theranostic nanoplatforms is a polymeric nanoparticle incorporated with photosensitizers.[48,55,121] Various types of photosensitizers have been used for cancer therapy because they generate cytotoxic singlet oxygen *via* an energy transfer to molecular oxygen under irradiation with light of an appropriate wavelength. Moreover, the photosensitizers have been employed for fluorescence imaging because they can also emit strong fluorescence signals upon irradiation. Therefore, over the last decade, photosensitizers have been considered as a potent theranostic agent capable of tumor imaging and therapy. However, photosensitizers pose intrinsic limitations for their *in vivo* applications. Most photosensitizers are scarcely soluble in physiological conditions; moreover, they may cause severe toxicity to the skin and eyes when they are exposed to the sun after systemic administration. Therefore, photosensitizers inevitably require delivery systems for their intravenous administration. Diverse polymeric nanoparticles have been employed as a delivery carrier for photosensitizers to date.

Weissleder and co-workers synthesized poly(lactic-*co*-glycolic acid) (PLGA) nanoparticles encapsulated with the photosensitizer *meso*-tetraphenylporpholactol as a theranostic nanoplatform.[48] When *meso*-tetraphenylporpholactol was encapsulated in the stable nanoparticles, the excitation state was highly quenched. In the quenched state, significant fluorescence signals or cytotoxic singlet oxygen was not produced. When the photosensitizers were released from the nanoparticles upon intracellular uptake, considerable fluorescence signals and phototoxicity were readily recovered. Consequently, with irradiation of visible light, the nanoparticles induced significant cytotoxicity to the cancer cells *in vitro* as well as *in vivo*, resulting in complete eradication of tumors in cancer xenografts. To the same end, Choi *et al.* proposed a polymer-based photodynamic therapy (PDT) agent composed of a biodegradable poly-L-lysine grafted with monomethoxy-polyethylene glycol (PGC) polymer backbone. The polymer backbone is coupled with multiple chlorine e6 (Ce6) pendants by specific peptide bonds that are degraded by the protease, cathepsin B (CaB), which is known to be up-regulated in various cancers.[49] In the intact physiological condition, the PDT agent does not show considerable fluorescence signals and singlet oxygen generation with light exposure due to the aggregation and self-quenching effect among the Ce6 molecules. However, after treatment of CaB, the singlet oxygen generation increased 6-fold compared to a control group. When nanoparticles were systemically administrated into HT1080 tumor-bearing mice, prominent fluorescence signals for PGC-Ce6 conjugates were detected in tumor tissues at 24h post-injection, indicating their passive accumulation *via* EPR effect and activation by CaB in the tumor regions.

Following irradiation of light, severe apoptosis and significant tissue loss were observed in the majority of the tumor, exhibiting remarkable toxicity to the cancer cells. These PDT-based theranostic approaches using polymeric nanoparticles containing photosensitizers can provide *in vivo* biodistribution or local concentration of PDT agents prior to treatment and then exert a significant anticancer effect to various cancers with illumination of light. Although such characteristics are effective towards cancer theranostics, PDT agents are greatly limited due to the low tissue penetration of light. Hence, clinical applications of such PDT-based strategies cannot be applied towards the detection and treatment of cancers within deep tissues.

Kwon and co-workers have investigated polymeric nanoparticles based on hydrophilic glycol chitosan (GC) conjugated with bile acid (BA) analogues as a multifunctional nanocarrier system.[50–53,55–57] Given their amphiphilic characteristics, GC-BA conjugates spontaneously form self-assembled nanoparticles composed of a GC shell and BA core in aqueous conditions.[122] Moreover, the GC-based nanoparticles (CNPs) can incorporate diverse signal emitters such as fluorophores[123] or MRI agents[124] to monitor their biodistribution *in vivo*. CNPs can also accommodate a wide variety of anticancer agents such as chemotherapeutics,[51–53,57] genes[56] and PDT agents[55] *via* physical encapsulation, chemical conjugation or electrostatic interaction. Poorly water-soluble anticancer drugs such as paclitaxel (PTX),[50] docetaxel,[51] camptothecin (CPT)[53] can be dispersed in aqueous conditions with the help of CNPs. In addition to improving solubility of hydrophobic drugs, CNP can also protect readily-hydolyzable drugs such as CPT from hydrolysis by its high encapsulation efficacy. *In vivo* biodistribution and tumor-targeting traits of drug-loaded CNPs were extensively examined using non-invasive/real-time near infrared fluorescence (NIRF) imaging techniques. For example, CNPs carrying the NIRF dye, Cy 5.5, and an anticancer drug PTX were prepared.[57] These nanoparticles were shown to circulate in the blood stream for up to 3 days and then be preferentially accumulated in tumor tissues *via* the EPR effect. At the tumor site, these nanoparticles exhibited 4-fold stronger signals than those in the normal tissues. The theranostic nanoparticles enabled simultaneous visualization and treatment of tumors in SCC7 tumor-bearing mouse models. Furthermore, they can also facilitate in monitoring the therapeutic efficacy *in vivo* (Fig. 7). Owing to their tumor specificity, they demonstrated considerable improvement in safety and anticancer efficacy in a variety of tumor-bearing mouse models over free drugs. These results suggest that polymeric nanoparticles can be used as an efficient platform for non-invasive/real-time tumor imaging, targeted cancer therapy, and monitoring of therapeutic responses for potential clinical applications.

Polymeric micelles have also been used as theranostic nanoplatforms. Rapoport *et al.*[61] reported a theranostic micelle system that integrated functions for ultrasound imaging and ultrasound-mediated chemotherapy. The system forms self-assembled nanostructures comprised of poly(ethylene glycol)-*block*-poly(L-lactide) (PEG-PLLA) polymeric micelles containing DOX and ultrasound imaging agent per-fluoropentane (PFP) with diameters ranging from 10 to 100 nm. At temperatures above the boiling temperature of PFP (29 °C), the nanoparticles generate nano/microbubbles which provide significant ultrasound contrast. Upon systemic administration, the nanoparticles accumulated into the tumor tissue and produced microbubbles. When therapeutic ultrasound was applied, the microbubbles collapsed and released DOX, which facilitates internalization of DOX into tumor cells and finally results in significant tumor regression in the mouse models (Fig. 8). More recently, polymersomes were encapsulated with both hydrophobically modified maghemite nanoparticles and DOX within their membrane as a potential theranostic nanocarrier for magnetic resonance (MR) imaging and magneto-chemotherapy.[63] The resulting polymersomes showed enhanced MR contrast properties. Upon radiofrequency magnetic

hyperthermia, drug release was triggered, implying the potential of the nanoplatform for the magneto-chemotherapy.

To date, a wide variety of sophisticated polymer nanoplatforms have been developed because it is easy to modify their functional groups, molecular weight, surface charge and other physicochemical properties. Given that they can accommodate therapeutic drugs and imaging agents, they are used to effectively locate and visualize tumors, deliver anticancer drugs to the tumor site and eradicate tumor cells. For these reasons, polymeric nanoparticles have shown great potential as cancer theranostics. However, most systems developed to date are still restricted in their clinical applications because of major concerns. Specifically, polymers have relatively low polydispersity index values; thus, it is hard to clearly characterize them in order to meet FDA regulatory requirements. And potentially, long circulation of polymeric nanocarriers may induce toxicity or hypersensitivity reactions.[125] Therefore, priority should be placed to study polymeric nanoparticle *in vivo* characteristics such as pharmacokinetics or maximum tolerated doses to successfully incorporate these nanoplatforms into clinical settings.

2.5. Silica nanoparticles

Recent advances in nanotechnology and material science have led to the development of silica nanoparticles (SNPs) that have promising physicochemical properties for biomedical applications.[5] Given that the SNPs are robust, bio-inert and easy to control in size and morphology, they have been employed as theranostic nanocarriers to deliver imaging agents and therapeutic molecules to the target site.[126] In an early study, Prasad and co-workers suggested SNPs (approximately 30 nm in diameter) encapsulated with a hydrophobic photosensitizer 2-devinyl-2-(1-hexyloxyethyl) pyropheophorbide (DHP) for photodynamic imaging and therapy.[127] The DHP-loaded SNPs (DHP-SNPs) were synthesized in the nonpolar core of micelles that surround DHP by hydrolysis of triethoxyvinylsilane. The resulting DHP-SNPs displayed strong fluorescence signals in aqueous medium, allowing for fluorescence bioimaging. Upon irradiation with light of a suitable wavelength, the DHP-SNPs produced cytotoxic singlet oxygen, which enables photodynamic therapy. The DHP-SNPs were readily internalized into the cancer cells (HeLa and UCI-107 cells); consequently, strong fluorescence signals were detected in the cytoplasm of the cancer cells treated with DHP-SNPs. Irradiation with NIR light of 650 nm resulted in significant destruction of the treated cancer cells. In a follow-up study, the Prasad group reported another theranostic application using SNPs containing both a two-photon dye 9,10-bis[4′-(4″-aminostyryl) styryl] anthracene (ASA) that shows strong fluorescence signals upon aggregation and a poorly water-soluble photosensitizer DHP.[42] Interestingly, upon strong two-photon excitation, the photosensitizer DHP was indirectly excited through intraparticle energy transfer from ASA dye aggregates in the cytoplasm of HeLa cells. Under two-photon irradiation, singlet oxygen was generated, inducing significant cytotoxicity to the cancer cell. These results demonstrate that SNPs loaded with photosensitizers hold great potential for both tumor imaging and therapy, *i.e.* cancer theranostics.

In particular, mesoporous silica nanoparticles (MSNPs) have been widely chosen as an attractive nanoplatform for drug delivery and bioimaging applications. Given their finely-controllable pores, considerable pore volume and large surface area, SNPs can incorporate or bind a high concentration (over 30%) of a wide variety of cargos like diverse imaging agents, *e.g.* fluorophores for optical imaging, superparamagnetic IONPs or paramagnetic gadolinium (Gd)-chelate for MR imaging and therapeutic drugs like DOX, CPT, PTX. Furthermore, SNPs can be functionalized with reversible molecular and supramolecular switches, permitting finely-controlled drug release triggered by various external/internal stimuli, *e.g.* pH changes, light irradiation, enzymes or magnetic field oscillation.[5,128] Recently, Ashley *et al.*[43] reported theranostic MSNPs covered with lipid bilayers

(protocells), which can store diverse cargos and functional molecules (Fig. 9). The protocells can incorporate both diagnostic agents and diverse therapeutic molecules that correspond to chemotherapeutic drugs, small interfering RNA and toxins. Moreover, the protocells can be modified with targeting peptides that selectively bind to human hepatocellular carcinoma with greater affinity than that to normal cells. In an attempt to promote endosomal escape and nuclear accumulation of given drugs, they also introduced a fusogenic peptide onto the surface of protocells. Combined with the capabilities to contain various cargos and to target cancer cells, the capability to deliver therapeutic cargos into the nucleus make them potential theranostic nanoplatforms, and lead to significant improvement (approximately a million times higher over liposomes) to overcome drug-resistant in human hepatocellular carcinoma cells. However, the theranostic SNPs are still in the early stage of development, and most studies on theranostic SNPs are confined to *in vitro* tests. Further, many key issues of concern, like *in vivo* biodistribution, toxicity or pharmacokinetics still remain to be addressed.

3. Current approaches and future perspectives

Theranostic nanoplatforms have harnessed beneficial approaches to deliver the synergistic effect on cancer theranostics. One of the main approaches is image-guided therapeutics. As we described above, *in vivo* biodistribution and tumor-targeting behavior of photosensitizer-based theranostic nanoparticles can be monitored by optical imaging techniques; also, based on the imaging results, laser irradiation can be aimed at the target site, leading to safe and effective photodynamic tumor ablation.[48,49] As another image-guided therapeutic system, the theranostic micelle loaded with PFP and DOX can be exempli-fied.[61] After intravenous injection, they accumulated in tumor tissues, generating ultrasound contrast. With irradiation of therapeutic ultrasound aimed at tumors, the drug release was triggered in the tumor tissues, causing significant toxicity to the cancer cells. Gold nanostructures and carbon nanotubes have also been used as image-guided cancer therapeutics. In these systems, imaging results provide the biodistribution or the tumor-targeting of drug and/or drug carriers, which can help clinicians to decide the irradiation site and the optimal therapeutic timing to ablate the tumor tissues.

The other essential approach in theranostics is therapeutic monitoring. Various theranostic systems are designed to monitor therapeutic efficacy in real time. The polymeric nanoparticle based on GC is a good example of therapeutic monitoring.[57] They showed excellent tumor targeting attributes due to the EPR effect, which enables both clear tumor imaging and tumor-targeted drug delivery. Consequently, the nanoparticle system significantly improved antitumor efficacy of anticancer drug PTX and reduced its undesirable side effects. Simultaneously, they monitored the therapeutic effect in real time, visualizing tumor growth or suppression behavior using NIRF imaging techniques. These theranostic nanoparticles showed great potential for cancer theranostics because they can provide clinicians with essential clues to make therapeutic decisions like if the treatment works well for patients and if the therapeutic regimens should continue. However, the information is still confined to the macroscopic phenomenon of tumor tissues; the majority of current theranostic nanoparticles cannot provide microscopic clues at the cellular level. To make accurate therapeutic decisions, more advanced theranostic systems that can monitor microscopic changes at the cellular level should be developed.

In the current article, we have highlighted diverse theranostic systems with integrated functions for cancer imaging and therapy. A wide variety of theranostic nanoplatforms that are based on diverse nanostructures, *i.e.* magnetic nanoparticles, carbon nanotubes, gold nanomaterials, polymeric nanoparticles, or silica nanoparticles showed great potential as cancer theranostics. However, although considerable efforts have been directed to the

development of theranostic nanoplatforms and approaches, theranostic nanoparticles have yet to be employed in a clinical setting. To date, most research on nanoparticle platforms as cancer theranostics has mainly focused on the development of multifunctional nanostructures; on the other hand, their clinical applications have not been sufficiently considered so far. For instance, numerous multifunctional nanoparticles can shuttle drugs and dyes to the target site, but the co-delivery in itself may not deliver significant synergistic effect for clinical applications. In addition, although specific types of theranostic nanoplatforms such as photosensitizer-based nanoparticles, gold nanostructures or carbon nanotubes can be harnessed for imaging-guided theranostics, their limited depth penetration may obstruct their clinical applications. Polymeric nanoparticles can enable targeted tumor-imaging/therapy and also facilitate monitoring the therapeutic effect; however, numerous issues of concern on safety and efficacy still remain. Consequently, to date, nanoparticle platforms have not shown significant potential for cancer theranostics in clinical settings. Moreover, a number of issues on the safety and efficacy of the theranostic nanostructures should be addressed. With that goal in mind, extensive discussion and multidisciplinary cooperation among clinicians, biologists, engineers, and material scientists should be required.

Acknowledgments

This work was supported by the Intramural Research Program (IRP) of the National Institutes of Biomedical Imaging and Bioengineering (NIBIB), National Institutes of Health (NIH). S. L. is partially supported by the NIH Pathway to Independence (K99/R00) Award.

References

1. American Cancer Society. Cancer Facts & Figures 2011. American Cancer Society; Atlanta: 2011.
2. Etzioni R, Urban N, Ramsey S, McIntosh M, Schwartz S, Reid B, Radich J, Anderson G, Hartwell L. Nat Rev Cancer. 2003; 3:243–252. [PubMed: 12671663]
3. Koo H, Huh MS, Sun IC, Yuk SH, Choi K, Kim K, Kwon IC. Acc Chem Res. 2011; 44:1018–1028. [PubMed: 21851104]
4. Al-Jamal WT, Kostarelos K. Acc Chem Res. 2011; 44:1094–1104. [PubMed: 21812415]
5. Ambrogio MW, Thomas CR, Zhao YL, Zink JI, Stoddart JF. Acc Chem Res. 2011; 44:903–913. [PubMed: 21675720]
6. Bardhan R, Lal S, Joshi A, Halas NJ. Acc Chem Res. 2011; 44:936–946. [PubMed: 21612199]
7. Ho D, Sun X, Sun S. Acc Chem Res. 2011; 44:875–882. [PubMed: 21661754]
8. Perry JL, Herlihy KP, Napier ME, Desimone JM. Acc Chem Res. 2011; 44:990–998. [PubMed: 21809808]
9. Chen XS. Theranostics. 2011; 1:1–2. [PubMed: 21547150]
10. Lukianova-Hleb EY, Oginsky AO, Samaniego AP, Shenefelt DL, Wagner DS, Hafner JH, Farach-Carson MC, Lapotko DO. Theranostics. 2011; 1:3–17. [PubMed: 21547151]
11. Zhu L, Xie J, Swierczewska M, Zhang F, Quan Q, Ma Y, Fang X, Kim K, Lee S, Chen X. Theranostics. 2011; 1:18–27. [PubMed: 21461134]
12. Yang M, Gao H, Zhou Y, Ma Y, Quan Q, Lang L, Chen K, Niu G, Yan Y, Chen X. Theranostics. 2011; 1:220–229. [PubMed: 21544226]
13. Zhang F, Zhu L, Liu G, Hida N, Lu G, Eden HS, Niu G, Chen X. Theranostics. 2011; 1:302–309. [PubMed: 21772927]
14. Fang C, Zhang M. J Controlled Release. 2010; 146:2–5.
15. Ferrari M. Nat Rev Cancer. 2005; 5:161–171. [PubMed: 15738981]
16. Park K, Lee S, Kang E, Kim K, Choi K, Kwon IC. Adv Funct Mater. 2009; 19:1553–1566.
17. Medarova Z, Pham W, Farrar C, Petkova V, Moore A. Nat Med. 2007; 13:372–377. [PubMed: 17322898]

18. Yang J, Lee CH, Ko HJ, Suh JS, Yoon HG, Lee K, Huh YM, Haam S. Angew Chem, Int Ed. 2007; 46:8836–8839.
19. Piao Y, Kim J, Na HB, Kim D, Baek JS, Ko MK, Lee JH, Shokouhimehr M, Hyeon T. Nat Mater. 2008; 7:242–247. [PubMed: 18278051]
20. Yu MK, Jeong YY, Park J, Park S, Kim JW, Min JJ, Kim K, Jon S. Angew Chem, Int Ed. 2008; 47:5362–5365.
21. Chen G, Chen W, Wu Z, Yuan R, Li H, Gao J, Shuai X. Biomaterials. 2009; 30:1962–1970. [PubMed: 19162315]
22. Cheng K, Peng S, Xu C, Sun S. J Am Chem Soc. 2009; 131:10637–10644. [PubMed: 19722635]
23. Das M, Mishra D, Dhak P, Gupta S, Maiti TK, Basak A, Pramanik P. Small. 2009; 5:2883–2893. [PubMed: 19856326]
24. Namiki Y, Namiki T, Yoshida H, Ishii Y, Tsubota A, Koido S, Nariai K, Mitsunaga M, Yanagisawa S, Kashiwagi H, Mabashi Y, Yumoto Y, Hoshina S, Fujise K, Tada N. Nat Nanotechnol. 2009; 4:598–606. [PubMed: 19734934]
25. Santra S, Kaittanis C, Grimm J, Perez JM. Small. 2009; 5:1862–1868. [PubMed: 19384879]
26. Xie J, Huang J, Li X, Sun S, Chen X. Curr Med Chem. 2009; 16:1278–1294. [PubMed: 19355885]
27. Chen W, Xu N, Xu L, Wang L, Li Z, Ma W, Zhu Y, Xu C, Kotov NA. Macromol Rapid Commun. 2010; 31:228–236. [PubMed: 21590896]
28. Liu G, Yang H, Zhang XM, Shao Y, Jiang H. Contrast Media Mol Imaging. 2010; 5:53–58. [PubMed: 20235146]
29. Xie J, Chen K, Huang J, Lee S, Wang J, Gao J, Li X, Chen X. Biomaterials. 2010; 31:3016–3022. [PubMed: 20092887]
30. Xie J, Wang J, Niu G, Huang J, Chen K, Li X, Chen X. Chem Commun. 2010; 46:433–435.
31. Amiri H, Mahmoudi M, Lascialfari A. Nanoscale. 2011; 3:1022–1030. [PubMed: 21152576]
32. Lartigue L, Innocenti C, Kalaivani T, Awwad A, del Sanchez Duque MM, Guari Y, Larionova J, Guerin C, Montero JL, Barragan-Montero V, Arosio P, Lascialfari A, Gatteschi D, Sangregorio C. J Am Chem Soc. 2011; 133:10459–10472. [PubMed: 21604803]
33. Liu G, Xie J, Zhang F, Wang Z, Luo K, Zhu L, Quan Q, Niu G, Lee S, Ai H, Chen X. Small. 2011; 7:2742–2749. [PubMed: 21861295]
34. Yallapu MM, Othman SF, Curtis ET, Gupta BK, Jaggi M, Chauhan SC. Biomaterials. 2011; 32:1890–1905. [PubMed: 21167595]
35. Quan Q, Xie J, Gao H, Yang M, Zhang F, Liu G, Lin X, Wang A, Eden HS, Lee S, Zhang G, Chen X. Mol Pharmacol. 2011; 8:1669–1676.
36. Loo C, Lowery A, Halas N, West J, Drezek R. Nano Lett. 2005; 5:709–711. [PubMed: 15826113]
37. Gobin AM, Lee MH, Halas NJ, James WD, Drezek RA, West JL. Nano Lett. 2007; 7:1929–1934. [PubMed: 17550297]
38. Ke H, Wang J, Dai Z, Jin Y, Qu E, Xing Z, Guo C, Yue X, Liu J. Angew Chem, Int Ed. 2011; 50:3017–3021.
39. Melancon MP, Elliott A, Ji X, Shetty A, Yang Z, Tian M, Taylor B, Stafford RJ, Li C. Invest Radiol. 2011; 46:132–140. [PubMed: 21150791]
40. Huang X, El-Sayed IH, Qian W, El-Sayed MA. J Am Chem Soc. 2006; 128:2115–2120. [PubMed: 16464114]
41. Day ES, Bickford LR, Slater JH, Riggall NS, Drezek RA, West JL. Int J Nanomed. 2010; 5:445–454.
42. Kim S, Ohulchanskyy TY, Pudavar HE, Pandey RK, Prasad PN. J Am Chem Soc. 2007; 129:2669–2675. [PubMed: 17288423]
43. Ashley CE, Carnes EC, Phillips GK, Padilla D, Durfee PN, Brown PA, Hanna TN, Liu J, Phillips B, Carter MB, Carroll NJ, Jiang X, Dunphy DR, Willman CL, Petsev DN, Evans DG, Parikh AN, Chackerian B, Wharton W, Peabody DS, Brinker CJ. Nat Mater. 2011; 10:389–397. [PubMed: 21499315]
44. Robinson JT, Welsher K, Tabakman SM, Sherlock SP, Wang H, Luong R, Dai H. Nano Res. 2010; 3:779–793. [PubMed: 21804931]

45. Kam NW, O'Connell M, Wisdom JA, Dai H. Proc Natl Acad Sci U S A. 2005; 102:11600–11605. [PubMed: 16087878]
46. Dhar S, Liu Z, Thomale J, Dai H, Lippard SJ. J Am Chem Soc. 2008; 130:11467–11476. [PubMed: 18661990]
47. Mashal A, Sitharaman B, Li X, Avti PK, Sahakian AV, Booske JH, Hagness SC. IEEE Trans Biomed Eng. 2010; 57:1831–1834. [PubMed: 20176534]
48. McCarthy JR, Perez JM, Bruckner C, Weissleder R. Nano Lett. 2005; 5:2552–2556. [PubMed: 16351214]
49. Choi Y, Weissleder R, Tung CH. Cancer Res. 2006; 66:7225–7229. [PubMed: 16849570]
50. Kim JH, Kim YS, Kim S, Park JH, Kim K, Choi K, Chung H, Jeong SY, Park RW, Kim IS, Kwon IC. J Controlled Release. 2006; 111:228–234.
51. Hwang HY, Kim IS, Kwon IC, Kim YH. J Controlled Release. 2008; 128:23–31.
52. Kim JH, Kim YS, Park K, Lee S, Nam HY, Min KH, Jo HG, Park JH, Choi K, Jeong SY, Park RW, Kim IS, Kim K, Kwon IC. J Controlled Release. 2008; 127:41–49.
53. Min KH, Park K, Kim YS, Bae SM, Lee S, Jo HG, Park RW, Kim IS, Jeong SY, Kim K, Kwon IC. J Controlled Release. 2008; 127:208–218.
54. Bryson JM, Fichter KM, Chu WJ, Lee JH, Li J, Madsen LA, McLendon PM, Reineke TM. Proc Natl Acad Sci U S A. 2009; 106:16913–16918. [PubMed: 19805101]
55. Lee SJ, Park K, Oh YK, Kwon SH, Her S, Kim IS, Choi K, Kim H, Lee SG, Kim K, Kwon IC. Biomaterials. 2009; 30:2929–2939. [PubMed: 19254811]
56. Huh MS, Lee SY, Park S, Lee S, Chung H, Lee S, Choi Y, Oh YK, Park JH, Jeong SY, Choi K, Kim K, Kwon IC. J Controlled Release. 2010; 144:134–143.
57. Kim K, Kim JH, Park H, Kim YS, Park K, Nam H, Lee S, Park JH, Park RW, Kim IS, Choi K, Kim SY, Kwon IC. J Controlled Release. 2010; 146:219–227.
58. Lee BS, Park K, Park S, Kim GC, Kim HJ, Lee S, Kil H, Oh SJ, Chi DY, Kim K, Choi K, Kwon IC, Kim SY. J Controlled Release. 2010; 147:253–260.
59. Santra S, Kaittanis C, Perez JM. Mol Pharmaceutics. 2010; 7:1209–1222.
60. Nasongkla N, Bey E, Ren J, Ai H, Khemtong C, Guthi JS, Chin SF, Sherry AD, Boothman DA, Gao J. Nano Lett. 2006; 6:2427–2430. [PubMed: 17090068]
61. Rapoport N, Gao Z, Kennedy A. J Natl Cancer Inst. 2007; 99:1095–1106. [PubMed: 17623798]
62. Kaida S, Cabral H, Kumagai M, Kishimura A, Terada Y, Sekino M, Aoki I, Nishiyama N, Tani T, Kataoka K. Cancer Res. 2010; 70:7031–7041. [PubMed: 20685894]
63. Sanson C, Diou O, Thevenot J, Ibarboure E, Soum A, Brulet A, Miraux S, Thiaudiere E, Tan S, Brisson A, Dupuis V, Sandre O, Lecommandoux S. ACS Nano. 2011; 5:1122–1140. [PubMed: 21218795]
64. Kenny GD, Kamaly N, Kalber TL, Brody LP, Sahuri M, Shamsaei E, Miller AD, Bell JD. J Controlled Release. 2011; 149:111–116.
65. Mikhaylov G, Mikac U, Magaeva AA, Itin VI, Naiden EP, Psakhye I, Babes L, Reinheckel T, Peters C, Zeiser R, Bogyo M, Turk V, Psakhye SG, Turk B, Vasiljeva O. Nat Nanotechnol. 2011; 6:594–602. [PubMed: 21822252]
66. Gianella A, Jarzyna PA, Mani V, Ramachandran S, Calcagno C, Tang J, Kann B, Dijk WJ, Thijssen VL, Griffioen AW, Storm G, Fayad ZA, Mulder WJ. ACS Nano. 2011; 5:4422–4433. [PubMed: 21557611]
67. Lukyanov AN, Elbayoumi TA, Chakilam AR, Torchilin VP. J Controlled Release. 2004; 100:135–144.
68. Park JW, Kirpotin DB, Hong K, Shalaby R, Shao Y, Nielsen UB, Marks JD, Papahadjopoulos D, Benz CC. J Controlled Release. 2001; 74:95–113.
69. Sapra P, Allen TM. Cancer Res. 2002; 62:7190–7194. [PubMed: 12499256]
70. Farokhzad OC, Cheng J, Teply BA, Sherifi I, Jon S, Kantoff PW, Richie JP, Langer R. Proc Natl Acad Sci U S A. 2006; 103:6315–6320. [PubMed: 16606824]
71. Farokhzad OC, Jon S, Khademhosseini A, Tran TN, Lavan DA, Langer R. Cancer Res. 2004; 64:7668–7672. [PubMed: 15520166]

72. Bies C, Lehr CM, Woodley JF. Adv Drug Delivery Rev. 2004; 56:425–435.
73. Minko T. Adv Drug Delivery Rev. 2004; 56:491–509.
74. Qian ZM, Li H, Sun H, Ho K. Pharmacol Rev. 2002; 54:561–587. [PubMed: 12429868]
75. Sahoo SK, Labhasetwar V. Mol Pharmaceutics. 2005; 2:373–383.
76. Lee RJ, Low PS. J Biol Chem. 1994; 269:3198–3204. [PubMed: 8106354]
77. Lu Y, Low PS. Adv Drug Delivery Rev. 2002; 54:675–693.
78. Eliaz RE, Szoka FC Jr. Cancer Res. 2001; 61:2592–2601. [PubMed: 11289136]
79. Xie J, Liu G, Eden HS, Ai H, Chen X. Acc Chem Res. 2011; 44:883–892. [PubMed: 21548618]
80. Liu G, Swierczewska M, Niu G, Zhang X, Chen X. Mol BioSyst. 2011; 7:993–1003. [PubMed: 21308113]
81. Nasongkla N, Shuai X, Ai H, Weinberg BD, Pink J, Boothman DA, Gao J. Angew Chem, Int Ed. 2004; 43:6323–6327.
82. Louie A. Chem Rev. 2010; 110:3146–3195. [PubMed: 20225900]
83. Ai H. Adv Drug Delivery Rev. 2011; 63:772–788.
84. Ibrahim NK, Desai N, Legha S, Soon-Shiong P, Theriault RL, Rivera E, Esmaeli B, Ring SE, Bedikian A, Hortobagyi GN, Ellerhorst JA. Clin Cancer Res. 2002; 8:1038–1044. [PubMed: 12006516]
85. Sparreboom A, Scripture CD, Trieu V, Williams PJ, De T, Yang A, Beals B, Figg WD, Hawkins M, Desai N. Clin Cancer Res. 2005; 11:4136–4143. [PubMed: 15930349]
86. Jeong H, Huh M, Lee SJ, Koo H, Kwon IC, Jeong SY, Kim K. Theranostics. 2011; 1:230–239. [PubMed: 21562630]
87. Liu G, Swierczewska M, Lee S, Chen X. Nano Today. 2010; 5:524–539. [PubMed: 22473061]
88. Wang Z, Liu G, Sun J, Wu B, Gong Q, Song B, Ai H, Gu Z. J Nanosci Nanotechnol. 2009; 9:378–385. [PubMed: 19441322]
89. Liu G, Wang Z, Lu J, Xia C, Gao F, Gong Q, Song B, Zhao X, Shuai X, Chen X, Ai H, Gu Z. Biomaterials. 2011; 32:528–537. [PubMed: 20869767]
90. Liu G, Xia C, Wang Z, Lv F, Gao F, Gong Q, Song B, Ai H, Gu Z. J Mater Sci: Mater Med. 2011; 22:601–606. [PubMed: 21279674]
91. Mikhaylov G, Mikac U, Magaeva AA, Itin VI, Naiden EP, Psakhye I, Babes L, Reinheckel T, Peters C, Zeiser R, Bogyo M, Turk V, Psakhye SG, Turk B, Vasiljeva O. Nat Nanotechnol. 2011; 7:594–602. [PubMed: 21822252]
92. Iijima S. Nature. 1991; 354:56–58.
93. Liu Z, Cai W, He L, Nakayama N, Chen K, Sun X, Chen X, Dai H. Nat Nanotechnol. 2007; 2:47–52. [PubMed: 18654207]
94. Liu Z, Davis C, Cai W, He L, Chen X, Dai H. Proc Natl Acad Sci U S A. 2008; 105:1410–1415. [PubMed: 18230737]
95. Bhirde AA, Liu G, Jin A, Iglesias-Bartolome R, Sousa AA, Leapman RD, Gutkind JS, Lee S, Chen X. Theranostics. 2011; 1:310–321. [PubMed: 21769298]
96. Liu Z, Robinsonb J, Tabakman S, Yang K, Da H. Mater Today. 2011; 14:316–323.
97. Liu Z, Chen K, Davis C, Sherlock S, Cao Q, Chen X, Dai H. Cancer Res. 2008; 68:6652–6660. [PubMed: 18701489]
98. Schipper ML, Nakayama-Ratchford N, Davis CR, Kam NW, Chu P, Liu Z, Sun X, Dai H, Gambhir SS. Nat Nanotechnol. 2008; 3:216–221. [PubMed: 18654506]
99. Liu Z, Tabakman S, Welsher K, Dai H. Nano Res. 2009; 2:85–120. [PubMed: 20174481]
100. Moon HK, Lee SH, Choi HC. ACS Nano. 2009; 3:3707–3713. [PubMed: 19877694]
101. Liu X, Tao H, Yang K, Zhang S, Lee ST, Liu Z. Biomaterials. 2011; 32:144–151. [PubMed: 20888630]
102. Singh PD, McCarthy R, Chaloin D, Hoebeke O, Partidos J, Briand CD, Prato JK, Bianco M, Kostarelos AK. J Am Chem Soc. 2005; 127:4388. [PubMed: 15783221]
103. Liu Y, Wu DC, Zhang WD, Jiang X, He CB, Chung TS, Goh SH, Leong KW. Angew Chem, Int Ed. 2005; 44:4782–4785.

104. Bartholomeusz G, Cherukuri P, Kingston J, Cognet L, Lemos R, Leeuw TK, Gumbiner-Russo L, Weisman RB, Powis G. Nano Res. 2009; 2:279–291. [PubMed: 20052401]
105. Kolosnjaj J, Szwarc H, Moussa F. Adv Exp Med Biol. 2007; 620:181–204. [PubMed: 18217344]
106. Porter AE, Gass M, Muller K, Skepper JN, Midgley PA, Welland M. Nat Nanotechnol. 2007; 2:713–717. [PubMed: 18654411]
107. Lam CW, James JT, McCluskey R, Arepalli S, Hunter RL. Crit Rev Toxicol. 2006; 36:189–217. [PubMed: 16686422]
108. Poland CA, Duffin R, Kinloch I, Maynard A, Wallace WA, Seaton A, Stone V, Brown S, Macnee W, Donaldson K. Nat Nanotechnol. 2008; 3:423–428. [PubMed: 18654567]
109. Daniel MC, Astruc D. Chem Rev. 2004; 104:293–346. [PubMed: 14719978]
110. Xia YN, Cobley CM, Chen JY, Cho EC, Wang LV. Chem Soc Rev. 2011; 40:44–56. [PubMed: 20818451]
111. Hu M, Chen J, Li ZY, Au L, Hartland GV, Li X, Marquez M, Xia Y. Chem Soc Rev. 2006; 35:1084–1094. [PubMed: 17057837]
112. Hirsch LR, Stafford RJ, Bankson JA, Sershen SR, Rivera B, Price RE, Hazle JD, Halas NJ, West JL. Proc Natl Acad Sci U S A. 2003; 100:13549–13554. [PubMed: 14597719]
113. Kim J, Park S, Lee JE, Jin SM, Lee JH, Lee IS, Yang I, Kim JS, Kim SK, Cho MH, Hyeon T. Angew Chem, Int Ed. 2006; 45:7754–7758.
114. Chen W, Bardhan R, Bartels M, Perez-Torres C, Pautler RG, Halas NJ, Joshi A. Mol Cancer Ther. 2010; 9:1028–1038. [PubMed: 20371708]
115. Tong L, Wei Q, Wei A, Cheng JX. Photochem Photobiol. 2009; 85:21–32. [PubMed: 19161395]
116. Choi KY, Chung H, Min KH, Yoon HY, Kim K, Park JH, Kwon IC, Jeong SY. Biomaterials. 2010; 31:106–114. [PubMed: 19783037]
117. Moon GD, Choi SW, Cai X, Li W, Cho EC, Jeong U, Wang LV, Xia Y. J Am Chem Soc. 2011; 133:4762–4765. [PubMed: 21401092]
118. Yavuz MS, Cheng Y, Chen J, Cobley CM, Zhang Q, Rycenga M, Xie J, Kim C, Song KH, Schwartz AG, Wang LV, Xia Y. Nat Mater. 2009; 8:935–939. [PubMed: 19881498]
119. Peer D, Karp JM, Hong S, Farokhzad OC, Margalit R, Langer R. Nat Nanotechnol. 2007; 2:751–760. [PubMed: 18654426]
120. Janib SM, Moses AS, MacKay JA. Adv Drug Delivery Rev. 2010; 62:1052–1063.
121. Lee SJ, Koo H, Jeong H, Huh MS, Choi Y, Jeong SY, Byun Y, Choi K, Kim K, Kwon IC. J Controlled Release. 2011; 152:21–29.
122. Kwon S, Park JH, Chung H, Kwon IC, Jeong SY, Kim IS. Langmuir. 2003; 19:10188–10193.
123. Na JH, Koo H, Lee S, Min KH, Park K, Yoo H, Lee SH, Park JH, Kwon IC, Jeong SY, Kim K. Biomaterials. 2011; 32:5252–5261. [PubMed: 21513975]
124. Nam T, Park S, Lee SY, Park K, Choi K, Song IC, Han MH, Leary JJ, Yuk SA, Kwon IC, Kim K, Jeong SY. Bioconjugate Chem. 2010; 21:578–582.
125. Park JH, Lee S, Kim JH, Park K, Kim K, Kwon IC. Prog Polym Sci. 2008; 33:113–137.
126. Rosenholm JM, Sahlgren C, Linden M. Nanoscale. 2010; 2:1870–1883. [PubMed: 20730166]
127. Roy I, Ohulchanskyy TY, Pudavar HE, Bergey EJ, Oseroff AR, Morgan J, Dougherty TJ, Prasad PN. J Am Chem Soc. 2003; 125:7860–7865. [PubMed: 12823004]
128. Klajn R, Stoddart JF, Grzybowski BA. Chem Soc Rev. 2010; 39:2203–2237. [PubMed: 20407689]

Biographies

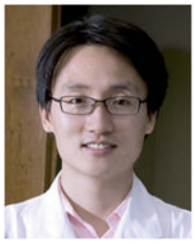

Ki Young Choi received his Ph. D. degree in 2011 from the Department of Life and Nanopharmaceutical Sciences at Kyung Hee Univ. in Korea. His Ph.D. project was focused on the development and application of various theranostic systems based on tumor-targetable nanoparticles for tumor imaging and therapy. In the summer of 2011, he joined Dr Xiaoyuan Chen's Laboratory of Molecular Imaging and Nanomedicine (LOMIN) in NIBIB at the NIH. His current research is focused on the development of potent theranostic systems for diagnosis and therapeutics of various diseases.

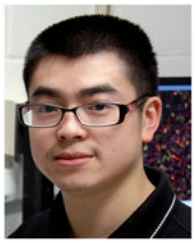

Gang Liu received his PhD in Biomedical and Bioengineering from Sichuan University in China, under the supervision of Professor Hua Ai. He joined the Laboratory of Molecular Imaging and Nanomedicine (LOMIN) of Dr Xiaoyuan Chen at the National Institute of Biomedical Imaging and Bioengineering (NIBIB), National Institutes of Health (NIH) as a postdoctoral researcher. His current research interests focus on the development of theranostic nanomedicine carrying both chemotherapeutics, gene therapeutics, and imaging tags.

Seulki Lee is a Group Leader of Theranostic Nanomedicine Section in the LOMIN at NIBIB, NIH. He received his PhD from the Department of Materials Science and Engineering at Gwangju Institute of Science and Technology (GIST) in Korea. He focused his training on nanomedicine and molecular imaging at the Molecular Imaging Program at Stanford (MIPS) under the supervision of Dr Xiaoyuan Chen. In 2009, he joined Dr Chen's new LOMIN at the NIBIB, NIH. With a background in nanomedicine and molecular imaging, his research aims to develop smart nanoplatforms for future diagnosis and therapy of various diseases with the emphasis on theranostics.

Xiaoyuan Chen received his PhD in chemistry from the University of Idaho in 1999. He joined the University of Southern California as an Assistant Professor of Radiology in 2002. He moved to Stanford University in 2004 and was promoted to Associate Professor in 2008. In 2009, he joined the Intramural Research Program of National Institute of Biomedical Imaging and Bioengineering as a tenured Senior Investigator and Chief of Laboratory of Molecular Imaging and Nanomedicine. He is interested in developing molecular imaging toolbox for early diagnosis of disease and monitoring therapy response. His lab puts special emphasis on high-sensitivity nanosensors and theranostic nanomedicine.

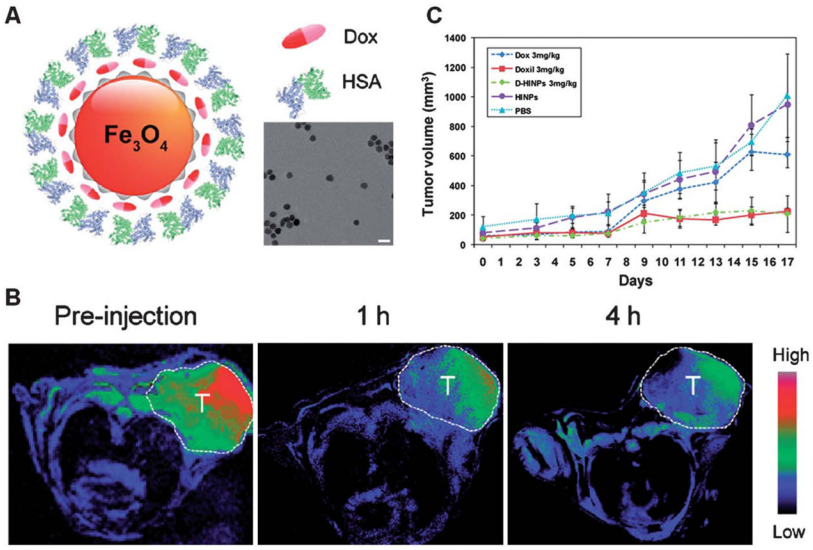

Fig. 1.

A. Schematic illustration and TEM image of the formation of D-HINPs. **B.** MR images taken before, and 1 and 4 h after the injection of D-HINPs. **C.** Tumor growth curves for treatment with D-HINPs, free DOX, Doxil, HINPs and PBS. Adapted with permission from Quan *et al.*[35] Copyright 2011, American Chemical Society.

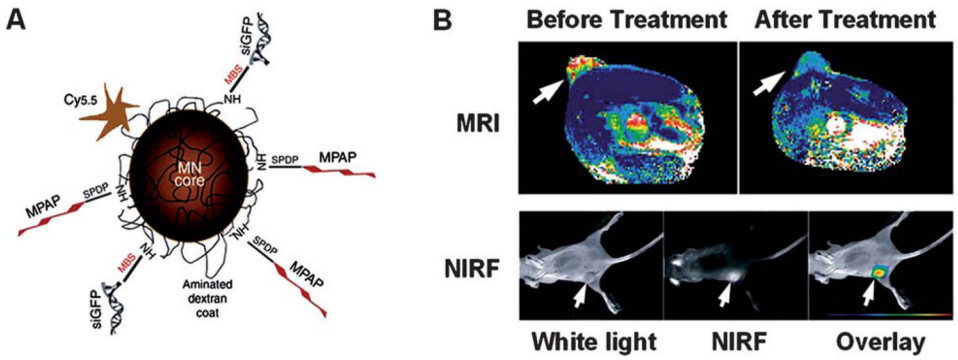

Fig. 2.

Multifunctional IONPs for *in vivo* dual-modality imaging and therapy. **A.** Schematic illustration of the multifunctional nanoparticles consisting of a magnetic nanoparticle labeled with Cy5.5, membrane translocation peptides (MPAP), and short-interfering ribose nucleic acid (siRNA) molecules. **B.** *In vivo* magnetic resonance imaging (MRI) of mice bearing subcutaneous tumors before and after treatment. High-intensity optical signal in the tumor confirmed the delivery of the nanoparticle. Adapted with permission from Medarova *et al.*[17] Copyright 2007, Nature Publishing Group.

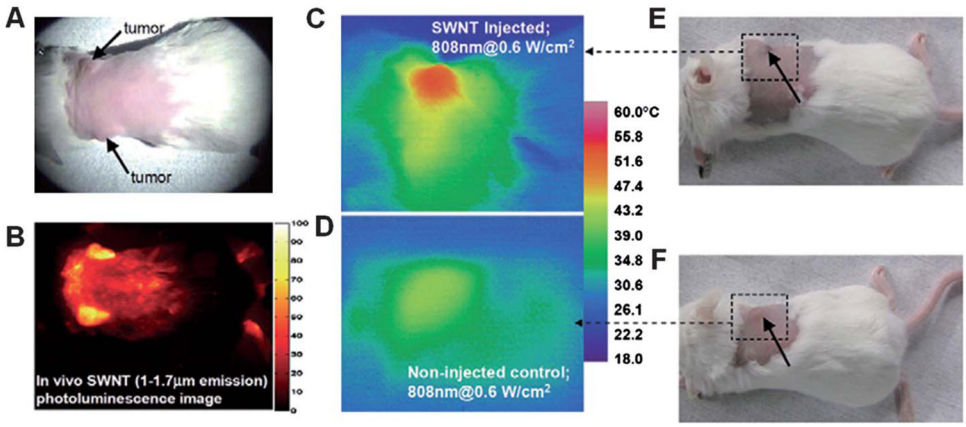

Fig. 3.

NIR fluorescence imaging guided photothermal therapy with SWNTs. A digital photo (**A**) and a NIR photoluminescence image (**B**) of a BALB/c mouse with two 4T1 tumors (indicated by arrows) taken after intravenous injection of SWNTs. IR thermal images of tumor-bearing mice (**C**) with and (**D**) without injection of SWNTs under 808 nm laser irradiation and the corresponding photos of mice before the NIR irradiation (**E,F**). Adapted with permission from Robinson *et al.*[44] Copyright 2010, Springer Science&Business Media and Tsinghua Press.

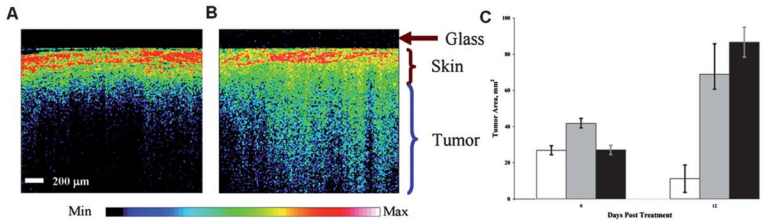

Fig. 4.

Representative OCT images from tumors of mice systemically injected with PBS (**A**) or with nanoshells (**B**). Representative OCT images from tumors of mice systemically injected with nanoshells. **C.** Tumor size before irradiation and 12 days post-irradiation of mice treated with nanoshell + NIR laser irradiation (white bar); PBS sham + NIR laser treatment (gray bar) or untreated control (black bar); values are average ± SEM. Adapted with permission from Gobin *et al.*[37] Copyright 2007, American Chemical Society.

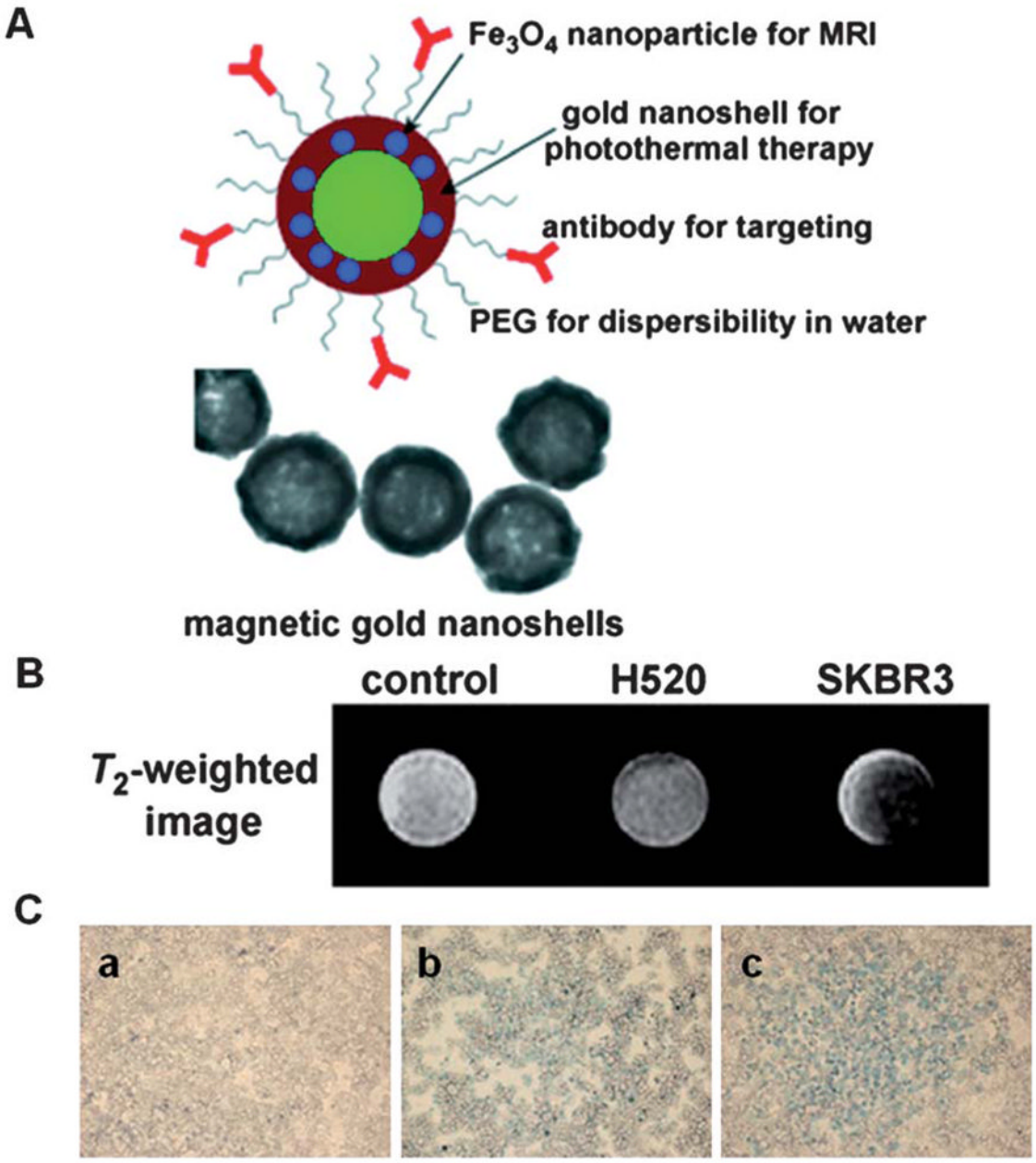

Fig. 5.

A. Schematic illustration and TEM images of the magnetic gold nanoshells (Mag-GNS) **B.** T2-weighted MR images of control SKBR3 cells, HER2/neu-negative H520 cells incubated with Mag-GNS-AbHER2/neu, and HER2/neu-positive SKBR3 cells incubated with Mag-GNS-AbHER2/neu. **D.** Optical microscope images of (a) control SKBR3 cells, (b) HER2/neu-negative H520 cells incubated with Mag-GNS-AbHER2/neu, and (c) HER2/neu-positive SKBR3 cells incubated with Mag-GNSAbHER2/neu after irradiation for 10 s with a femtosecond-pulse laser (with a wavelength of 800 nm and a beam diameter of 1 mm) and subsequent staining with trypan blue. Adapted with permission from Kim *et al.*[113] Copyright 2006, John Wiley & Sons, Inc.

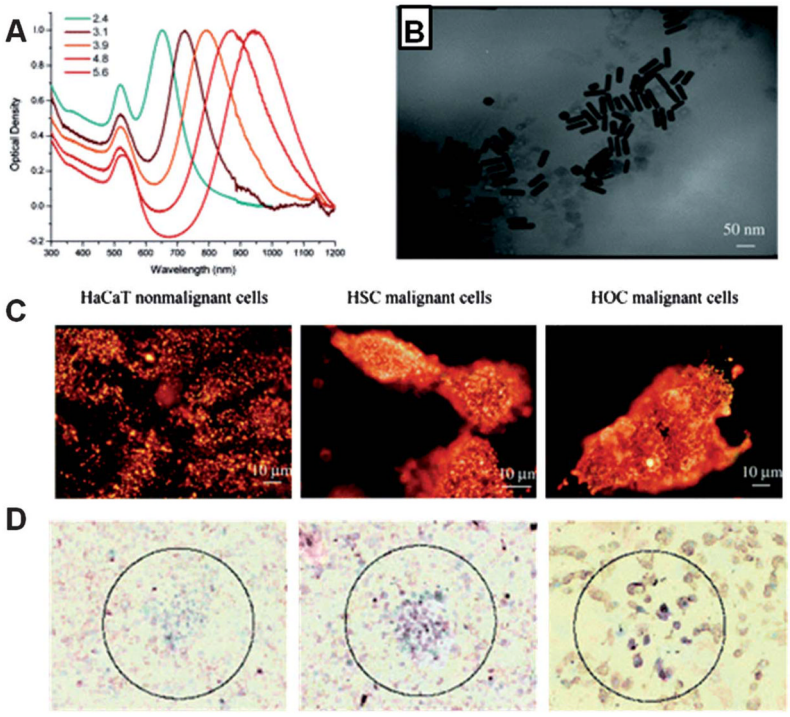

Fig. 6.

A. Surface plasmon absorption spectra of gold nanorods of different aspect ratios, showing the sensitivity of the strong longitudinal band to the aspect ratios of the nanorods. **B.** TEM image of nanorods of aspect ratio of 3.9, the absorption spectrum of which is shown as the orange curve in panel A. **C.** Light scattering images of anti-EGFR/Au nanorods after incubation with cells for 30 min at room temperature. **D.** Selective photothermal therapy of cancer cells with anti-EGFR/Au nanorods incubated. The circles show the laser spots on the samples. Adapted with permission from Huang *et al.*[40] Copyright 2006, American Chemical Society.

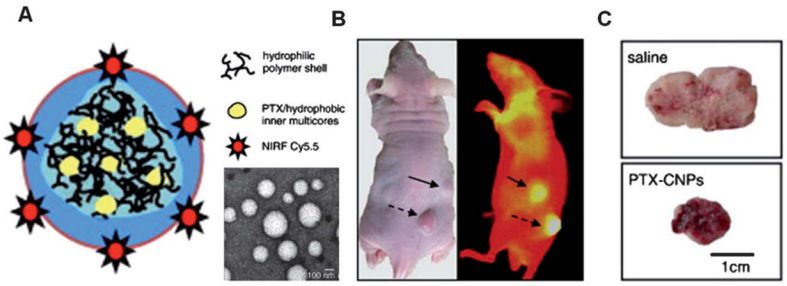

Fig. 7.

A. Schematic diagram and TEM image of chitosan-based nanoparticles (CNPs). **B.** *In vivo* images of tumor specificity. The black arrow indicates intravenous injection of Cy5.5-labeled PTX-CNPs. **C.** Representative images of excised tumors treated with saline and PTX-CNPs for 18 days. Adapted with permission from Kim *et al.*[57] Copyright 2010 Elsevier Ltd.

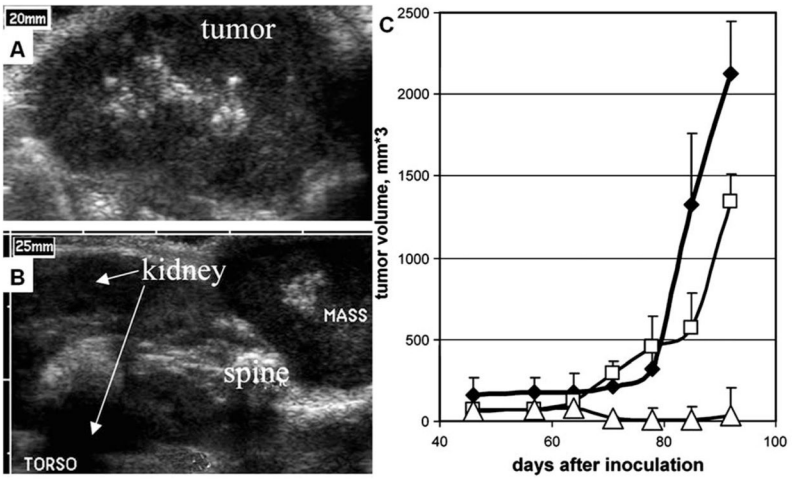

Fig. 8.

A. B-mode ultrasound image of MDA MB231 human breast cancer tumor in a nude mouse after intravenous injection of PEG-PLLA/perfluoropentane microbubble formulation. Image taken 4.5 h after injection. **B**. Trans-torso image of the same mouse showing the tumor (designated as “mass”), kidneys, and spine. **C.** Tumor growth curves for control mice (filled diamonds); mice treated by four tail vein injections of DOX-loaded microbubbles administered twice weekly without ultrasound (open squares); and mice treated by the same regimen combined with tumor sonication (open triangles). n = 3–5. Adapted with permission from Rapoport *et al.*[61] Copyright 2007 Oxford University Press.

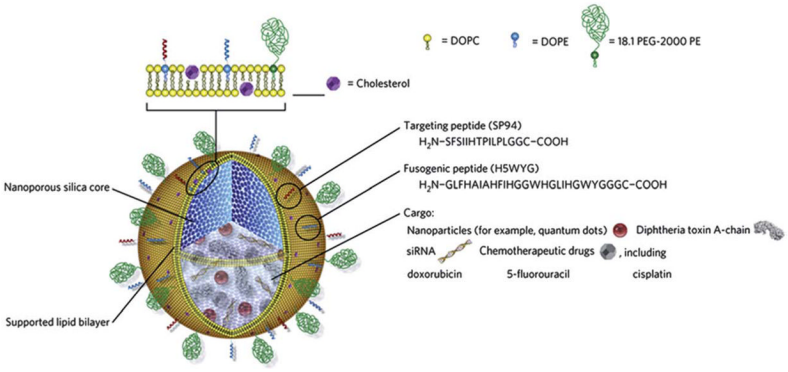

Fig. 9.

Schematic illustration of the nanoporous particle-supported lipid bilayer, depicting the disparate types of therapeutic and diagnostic agent that can be loaded within the nanoporous silica core. Adapted with permission from Ashley *et al.*[43] Copyright 2011, Nature Publishing Group.

Table 1

Representative nanoplatforms, imaging modalities and therapeutics used in theranostic nanoparticles[a]

Nanoplatforms	Imaging modalities	Therapeutics	Ref.
Inorganic nanoplatforms			
Magnetic nanoparticle	MRI, OI(NIRFI)	CMT(DOX, MTX, curcumin, cisplatin), BT(pDNA, siRNA), HTT	17–35
Gold nanoshell	OI(DFI), US, MRI	PTT	36–39
Gold nanorod	OI(DFI)	PTT	40
Gold nanoparticle	OI(PLI)	PTT	41
Slica nanoparticles	OI(NIRFI, PDI)	CMT(DOX), BT(siRNA, protein), PDT	42, 43
Organic nanoplatforms			
Carbon nanotube	OI (PLI), RS, MWD	PTT, HTT, CMT(PtD)	44–47
Polymeric nanoparticle	MRI, PET, OI(NIRFI, PDI)	CMT(PTX, CPT, DTX, DOX, cisplatin), BT(pDNA, siRNA, protein), PDT	48–59
Polymeric micelle	MRI, USI	CMT(DOX, PtD)	60–62
Polymersome	MRI	CMT(DOX)	63
Liposome	MRI	BT(peptide, siRNA)	64, 65
Nanoemulsion	MRI, OI(NIRFI)	CMT(PAV)	66

[a]**Abbrev.: MRI**: magnetic resonance imaging, **PET**: positron emission tomography, **USI**: ultrasound imaging, **OI**: optical imaging, **NIRFI**: near infrared fluorescence imaging, **PDI**: photodynamic imaging, **PAI**: photoacoustic imaging, **DFI**: dark field imaging, **RS**: Raman spectroscopy, **PLI**: photoluminescence imaging, **CMT**: chemotherapy, **DOX**: doxorubicin, **PTX**: paclitaxel, **CPT**: camptothecin, **DTX**: docetaxel, **PAV**: prednisolone acetate valerate, **PtD**: platinum anticancer drug, **MTX**: metotrexate, **BT**: biotherapeutics, **MWD**: microwave detection, **PDT**: photodynamic therapy, **PTT**: photothermal therapy, **HTT**: hyperthermal therapy.